Geophysical Research Letters

RESEARCH LETTER
10.1029/2019GL086676

Explicit IMF B_y Dependence in Geomagnetic Activity: Modulation of Precipitating Electrons

L. Holappa[1], **T. Asikainen**[1], **and K. Mursula**[1]

[1]ReSoLVE Centre of Excellence, Space Physics and Astronomy Research Unit, University of Oulu, Oulu, Finland

Key Points:
- Fluxes of energetic electrons precipitating into atmosphere are strongly dependent on the sign and amplitude of IMF B_y
- This IMF B_y effect on electron fluxes is strong around midnight and at dawn but weak at dusk
- This IMF B_y effect is expected to modulate ionospheric conductivity and to affect a similar effect in geomagnetic activity

Correspondence to:
L. Holappa,
lauri.holappa@oulu.fi

Citation:
Holappa, L., Asikainen, T., & Mursula, K. (2020). Explicit IMF B_y-dependence in geomagnetic activity: Modulation of precipitating electrons. *Geophysical Research Letters*, *47*, e2019GL086676. https://doi.org/10.1029/2019GL086676

Received 17 DEC 2019
Accepted 3 FEB 2020
Accepted article online 6 FEB 2020

Abstract The most important driver of geomagnetic activity is the north–south (B_z) component of the interplanetary magnetic field (IMF), which dominates the solar wind-magnetosphere coupling and all solar wind coupling functions. While the east–west (B_y) IMF component is also included in most coupling functions, its effect is always assumed to be symmetric with respect of its sign. However, recent studies have shown that, for a fixed value of any coupling function, geomagnetic activity is stronger for $B_y > 0$ than for $B_y < 0$ in Northern Hemisphere winter. In Southern Hemisphere winter, the dependence on the B_y sign is reversed. In this paper, we use measurements of National Oceanic and Atmospheric Administration Polar-Orbiting Operational Environmental Satellites to show that the flux of magnetospheric electrons precipitating into the atmosphere also exhibits an explicit B_y dependence. This B_y dependence is strong in the midnight and dawn sectors where it causes a related B_y effect in the westward electrojet and geomagnetic activity by modulating ionospheric conductivity.

1. Introduction

Short-term variability of the Earth's magnetic field, also known as geomagnetic activity, is one of the most significant manifestations of space weather. Geomagnetic activity is caused by various electric currents in the near-Earth space, maintained by the interaction between solar wind and the magnetosphere. The most significant factor contributing to geomagnetic activity is the north–south (B_z) component of the interplanetary magnetic field (IMF), measured in the Geocentric Solar Magnetospheric coordinate system. While the east–west (B_y) IMF component is also known to contribute to the reconnection rate (Laitinen et al., 2007; Sonnerup, 1974), its effect is symmetric with respect to its sign, that is, if other solar wind parameters are held constant, the reconnection rate does not change if the sign of B_y is reversed. This symmetric effect of IMF B_y is included in most solar wind-magnetosphere coupling functions, such as the Newell universal coupling function (Newell et al., 2007)

$$d\Phi_{MP}/dt = v^{4/3}B_T^{2/3}\sin^{8/3}(\theta/2), \quad (1)$$

where v is solar wind speed, $B_T = \sqrt{B_z^2 + B_y^2}$, and $\theta = \arctan(B_y/B_z)$ is the so-called IMF clock angle.

Recent observations of the geomagnetic field by polar-orbiting satellites (Friis-Christensen et al., 2017; Smith et al., 2017) found that the westward auroral electrojet in both hemispheres is more intense in Northern Hemisphere (NH) winter for $B_y > 0$ than for $B_y < 0$. For Southern Hemisphere (SH) winter, the effect of B_y is opposite: the westward electrojet is more intense for $B_y < 0$ than for $B_y > 0$. Holappa and Mursula (2018) quantified this new, *explicit*B_y effect in detail and showed that during NH winter solstice, for a given value of $d\Phi_{MP}/dt$, the value of the *AL* index (measuring the NH westward electrojet) is 40–50% greater for $B_y > 0$ than for $B_y < 0$. During NH summer, the *AL* index is about 10% stronger for $B_y < 0$ than for $B_y > 0$. Holappa and Mursula (2018) also studied the B_y dependence of the SH westward electrojet using the *K* index at Syowa station in Antarctica and found a strong B_y effect (higher *K* index for $B_y < 0$) in SH winter and a weak B_y effect in SH summer. Thus the B_y effect in geomagnetic activity has the same sign globally, but it is clearly stronger in local winter than in local summer. Holappa and Mursula (2018) also showed that the B_y effect maximizes when the Earth's dipole axis points towards midnight (5 UT in NH). This combined seasonal/UT dependence suggests that the B_y effect in ionospheric currents may work most efficiently under low ionospheric conductivity.

This explicit B_y effect is currently not included in any space weather prediction models. However, Holappa et al. (2019) showed that the B_y effect strongly affects geomagnetic activity even at subauroral latitudes

during geomagnetic storms driven by coronal mass ejections. Thus, inclusion of the B_y effect to models predicting space weather is important for the future predictions of space weather hazards, such as geomagnetically induced currents.

The physical mechanism of the B_y effect in geomagnetic activity is not yet known. Friis-Christensen et al. (2017) suggested that IMF B_y modulates the strength of the substorm current wedge, which probably makes the largest contribution to the *AL* index. While this mechanism is consistent with observations (Friis-Christensen et al., 2017; Holappa & Mursula, 2018; Holappa et al., 2019), it is still unclear how IMF B_y is connected to the substorm current wedge. In principle, in order to be able to modulate ionospheric currents, IMF B_y must modulate either the ionospheric electric fields or ionospheric conductivity or both. Radar studies (Pettigrew et al., 2010; Thomas & Shepherd, 2018) have shown that the cross-polar cap potential exhibits a qualitatively similar B_y dependence as high-latitude geomagnetic activity, indicating a B_y dependence in ionospheric electric fields that may contribute to ionospheric currents. A recent study gives evidence that there is an explicit B_y dependence also in polar cap area, indicating a possible explicit B_y effect in the dayside reconnection rate (Reistad et al., 2020). This is consistent with the above radar observations since the modulation of the reconnection rate would modulate magnetospheric convection and electric fields mapped into the ionosphere. The detailed mechanism of the B_y effect in the dayside reconnection is not well understood. However, several studies have shown that the geometry of the reconnection X-line varies with (seasonally changing) dipole tilt angle and IMF B_y (Liu et al., 2012; Park et al., 2006; Zhu et al., 2015). The X-line may also be split into the two hemispheres if the IMF vector is dominated by the B_y component (Connor et al., 2015; Trattner et al., 2012). More research is needed to identify which of these produce the B_y dependence. However, it is important to note that the B_y dependence of the dayside reconnection rate alone does not explain why the B_y effect in geomagnetic activity is strong only in local winter (Holappa & Mursula, 2018; Smith et al., 2017).

In addition to electric fields, ionospheric currents (such as the substorm current wedge) also depend on ionospheric conductivity, which is controlled by solar illumination and the precipitation of magnetospheric particles into the ionosphere. The goal of this paper is to study whether there is a B_y effect in the flux of magnetospheric particles precipitating into high-latitude ionosphere. Understanding the relation between IMF B_y and particle precipitation is an important step toward a better understanding of the B_y effect, as particle precipitation is an important source of ionospheric conductivity (especially in the nightside ionosphere), thus strongly contributing to the westward electrojet.

2. Energetic Electron Measurements

In this paper, we utilize the long database of magnetospheric energetic electron measurements by the Medium Energy Proton and Electron Detector instruments on board National Oceanic and Atmospheric Administration (NOAA) Polar-Orbiting Operational Environmental Satellites (NOAA15–NOAA19). These fluxes have been calibrated and corrected for instrument efficiency and cross contamination by energetic protons to form a homogenous long-term data set of energetic electron fluxes (Asikainen & Mursula, 2013). In this paper, we analyze the flux of electrons in the lowest energy channel (>30 keV) precipitating into the atmosphere (0° detector). The polar orbits of different NOAA satellites are on different magnetic local time (MLT) planes and vary slowly with time (Asikainen & Ruopsa, 2019), which allows us to study the B_y effect in different MLT sectors. In this paper, we analyze the electron flux data in three different (8 hr wide) MLT bins: 20-04 MLT (night), 04-12 MLT (dawn), and 12-20 MLT (dusk), in order to study possible MLT dependence of the B_y effect. The motivation for using such a wide MLT bin width is to ensure sufficient statistics in all bins.

3. IMF By-Effect in Electron Fluxes

In order to test whether there is an explicit IMF B_y-effect in the flux of precipitating electrons, we use a similar methodology as Holappa and Mursula (2018). Figures 1a and 1b show the average fluxes (F) of precipitating electrons for different values of IMF B_y and $d\Phi_{MP}/dt$ around NH winter solstice (December 21 ±30 days) separately for NH and SH, respectively. (Figure 1 shows fluxes in a logarithmic scale. The original fluxes are given in the units $1/[\mathrm{cm}^2\ \mathrm{sr\,s}]$.) The electron fluxes in Figure 1 are averaged over 20-04 MLT and ±(50° … 70°) corrected geomagnetic latitude using all available data from NOAA15–NOAA19 satellites between 1998 and 2017. The coupling function $d\Phi_{MP}/dt$ is normalized by its long-term average $\langle d\Phi_{MP}/dt\rangle$

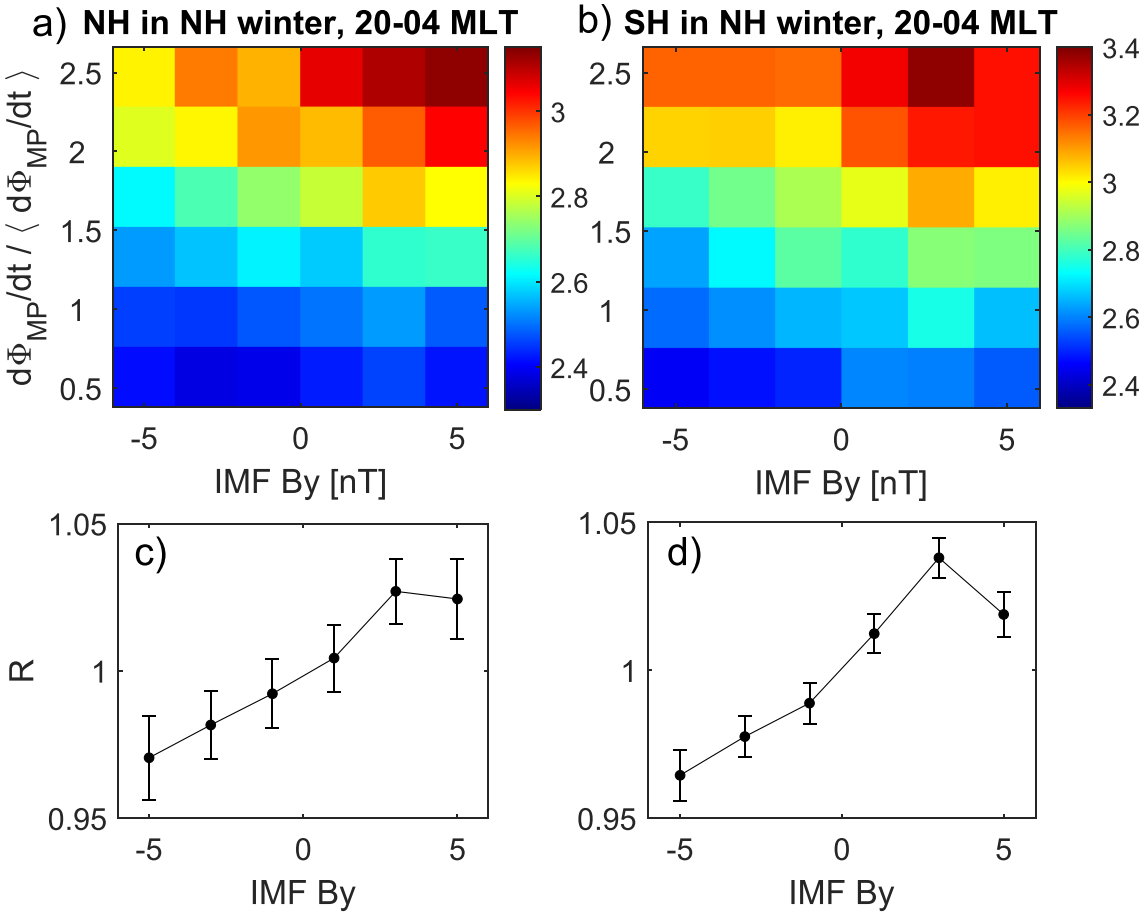

Figure 1. Average logarithmic flux ($\log_{10}F$) of precipitating electrons for different values of the solar wind coupling function $d\Phi_{MP}/dt$ and IMF B_y in NH winter solstice ±30 days in (a) Northern Hemisphere (50–70° CGM latitude) and (b) Southern Hemisphere (−50° to −70° CGM latitude). The values of $d\Phi_{MP}/dt$ are normalized by the average of the coupling function ($\langle d\Phi_{MP}/dt \rangle$) in 2003–2017. For a given value of $d\Phi_{MP}/dt$, the electron flux is higher for $B_y > 0$ than for $B_y < 0$ in both hemispheres, that is, electron fluxes show an explicit IMF B_y dependence. Panels (c) and (d) depict the normalized column averages (R) of the flux matrices in panels (a) and (b), quantifying the explicit B_y dependence for NH and SH, respectively. Vertical bars denote the 2σ standard errors.

calculated over all data in 1998–2017. Figures 1a and 1b clearly show that for a given value of $d\Phi_{MP}/dt$, the flux of precipitating electrons in NH winter is greater for $B_y > 0$ than for $B_y < 0$ in both hemispheres. This explicit B_y dependence is very similar in both hemispheres. This indicates that the B_y effect in >30-keV electrons is not related to polar rain, that is, precipitation of electrons of few hundred eV on the northern polar cap for $B_y > 0$ (away sector) and for the southern polar cap for $B_y < 0$ (toward sector) (Fairfield & Scudder, 1985). Note that the overall electron flux in SH is somewhat greater than in NH (different color scales in Figures 1a and 1b), probably due to the South Atlantic anomaly and other hemispheric asymmetries in the Earth's magnetic field (Meredith et al., 2011; Vampola & Gorney, 1983).

We further quantify the strength of the explicit B_y dependence in Figures 1c and 1d that show weighed column averages (R) of the flux matrices in Figures 1a and 1b together with their 2σ errors. Before calculating the column means, each row is first normalized (divided) by its mean. This ensures that fluxes corresponding to different values of the solar wind coupling function are weighed equally. Figures 1c and 1d show that R increases rather linearly with IMF B_y in both hemispheres. The ratio $R(B_y \geq 3\ nT)/R(B_y \leq -3\ nT)$ is about 1.05 for NH (1.06 for SH). This is quite significant in linear scale since, for example, for a flux of $\log_{10}F = 3$, this corresponds to about 40% relative effect in NH (50% in SH). The relative effect grows with the level of electron precipitation: for the two uppermost rows in the flux matrix with the greatest $d\Phi_{MP}/dt$ (and electron fluxes), the relative effect is about 60% in NH (50% in SH). This is consistent with the study of Shue et al. (2001) who found that the relative impact of IMF B_y on auroral brightness increases with increasing southward B_z. Interestingly, the $B_y$effect in the electron fluxes is roughly equally strong in the winter and

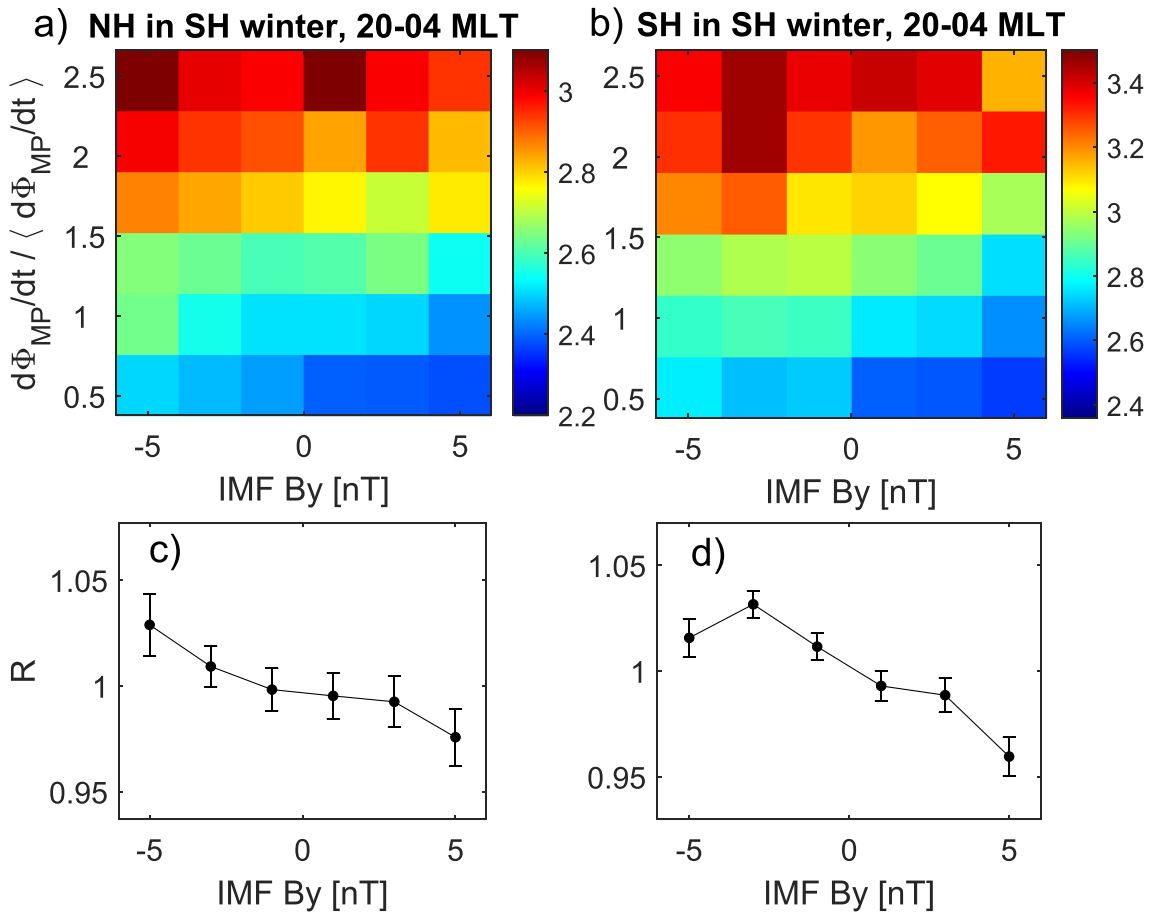

Figure 2. Same as Figure 1 but for SH winter (NH summer) solstice ±30 days.

summer hemispheres (the difference being statistically insignificant). This winter–summer symmetry of the B_y effect is not seen in geomagnetic activity (Holappa & Mursula, 2018; Smith et al., 2017).

Figures 2a and 2b are similar to Figures 1a and 1b but show the electron fluxes for NH summer (June 21 ± 30 days). Figures 2a and 2b show that in SH winter (NH summer), the flux of precipitating electrons is greater for $B_y < 0$ than for $B_y > 0$ in both hemispheres. Thus the dependence on the sign of B_y is opposite for NH winter and SH winter. Again, the overall electron flux is greater in SH than in NH, but the relative strength of the B_y effect is roughly the same in both hemispheres (see Figures 2c and 2d). The ratio $R(B_y \leq -3\ nT)/R(B_y \geq 3\ nT)$ is about 1.04 in NH (1.05 in SH). For a flux $\log_{10}F = 3$, this corresponds to about 30% effect in linear scale in NH (40% in SH). These ratios are quite close to those obtained from Figures 1c and 1d, indicating that the explicit B_y effect is roughly equally strong in magnitude during both solstices.

Figures 3 and 4 show the electron fluxes in NH winter for dawn/prenoon (04-12 MLT) and dusk/afternoon (12-20 MLT) sectors, respectively. The electron fluxes in the dawn sector are slightly higher than in the midnight sector (Figures 1 and 2) and much higher than in the dusk sector (note the different color scales). This is due to the fact that energetic electrons injected into inner magnetosphere are partly precipitated into the atmosphere mostly in the dawn sector before drifting further on to dusk (Lam et al., 2010). The B_y effect in the dawn sector in NH winter (Figure 3) has the same magnitude as in the midnight sector (Figure 1) with $R(B_y \geq 3\ nT)/R(B_y \leq -3\ nT)$ of about 1.05 in NH and 1.06 in SH (40% and 50% in linear scale for $\log_{10}F = 3$, respectively). The B_y effect at dawn (Figure 3) is also remarkably symmetric between the winter and summer hemispheres. Even though the dusk electron fluxes are low, they do show a weak B_y dependence in Figure 4 in both hemispheres. However, R does not increase linearly with B_y, and the ratio $R(B_y \leq -3\ nT)/R(B_y \geq 3\ nT)$ is about 1.02 for NH (1.03 for SH). For a typical dusk electron flux ($\log_{10}F = 2.5$), this corresponds to about 10% effect in NH (20% in SH) in linear scale. Thus the explicit B_y dependence in the dusk sector is significantly weaker than in the two other sectors.

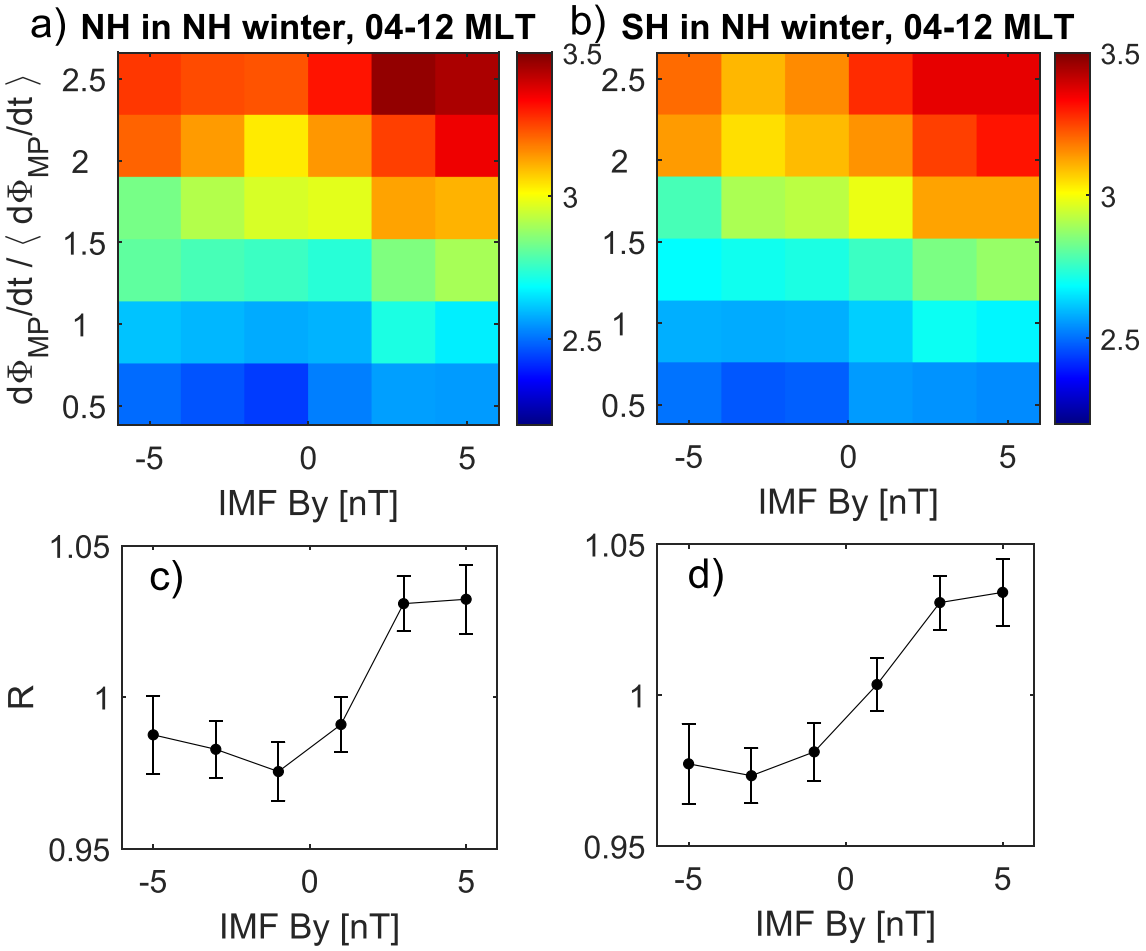

Figure 3. Same as Figure 1 but for dawn (04-12 MLT).

4. Discussion and Conclusions

In this paper, we have shown that for a given fixed value of Newell solar wind-coupling function, the IMF B_y component affects the flux of energetic (>30 keV) electrons precipitating into the atmosphere in the latitude range of ±(50–70°) corrected geomagnetic latitude. This *explicit*B_y effect exhibits a systematic seasonal dependence: in NH winter, the flux of precipitating electrons is greater for $B_y > 0$ than for $B_y < 0$ in both hemispheres. In SH winter, the dependence on the B_y sign is reversed. We found that the magnitude of the explicit B_y effect is roughly equal in both hemispheres and solstices.

Previous studies (Holappa & Mursula, 2018; Smith et al., 2017) have shown that the explicit B_y effect in *geomagnetic activity* is much stronger in the winter hemisphere than in the summer hemisphere. Furthermore, Holappa and Mursula (2018) showed that the B_y effect in NH geomagnetic activity maximizes at 5 UT, when the Earth's magnetic dipole axis points towards midnight and the northern auroral region is maximally in darkness. These results imply that the B_y effect in geomagnetic activity works most efficiently under low ionospheric conductivity.

In contrast to geomagnetic activity, we have found that the B_y dependence of precipitating electrons is roughly equally strong in the winter and summer hemispheres. Thus the B_y effect to ionospheric conductivity, through the ionization by electron precipitation, is equally strong in the winter and summer hemispheres. However, in local winter, under low photoionization, particle precipitation, and thereby IMF B_y control, a relatively large fraction of the total (photoionization + precipitation) conductivity. We suggest that this explains why the B_y effect in geomagnetic activity is relatively strong in local winter than summer.

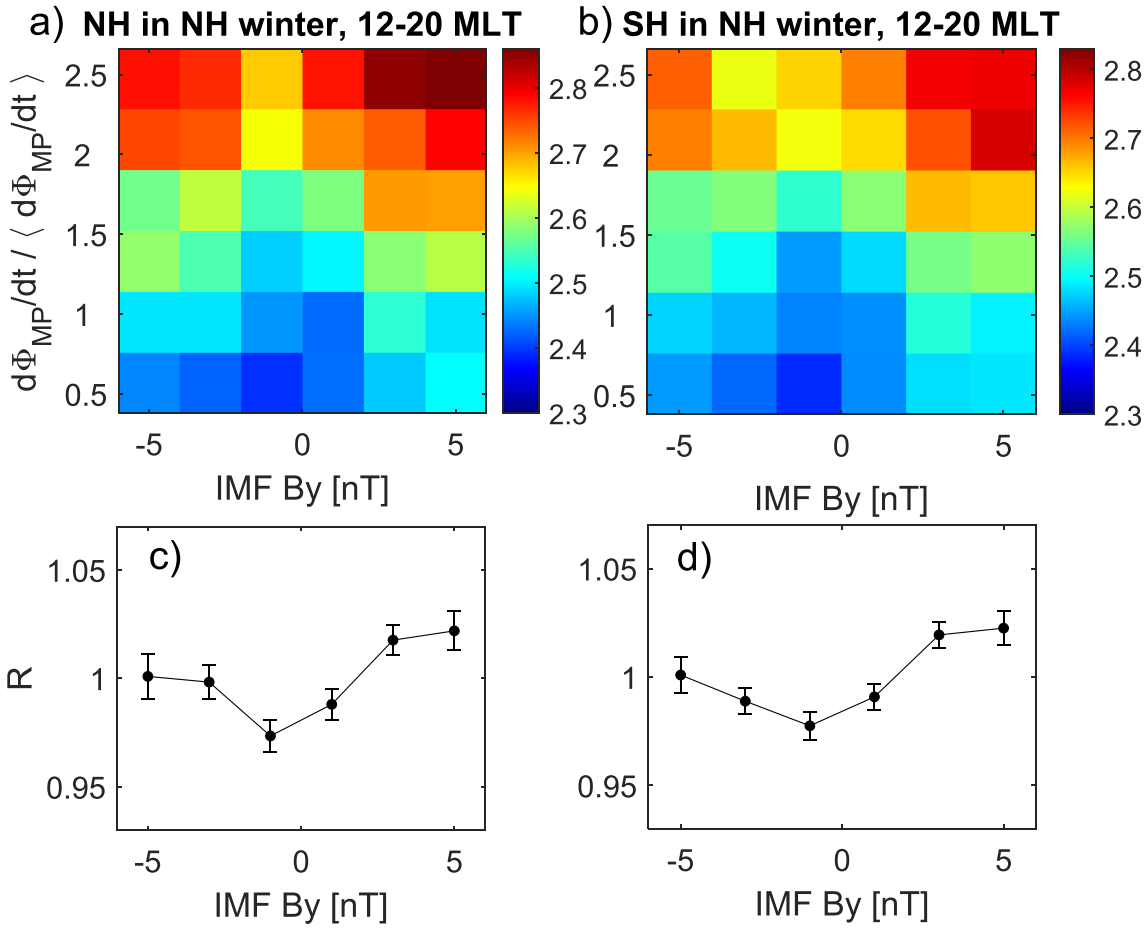

Figure 4. Same as Figure 1 but for dusk (12-20 MLT).

In this paper, we also showed that while the B_y effect in the flux of precipitating electrons is strong in the midnight (20-04 MLT) and dawn (04-12 MLT) sectors, it is weak in the dusk sector (12-20 MLT). Moreover, we found that the overall level of electron precipitation is much lower in the dusk sector than in the two other sectors. This implies that IMF B_y modulates ionospheric conductivity significantly in midnight and dawn sectors but much less in the dusk sector. This is in excellent agreement with the earlier finding that the B_y effect modulates the westward electrojet (located in the midnight and dawn sectors) but not the eastward electrojet located in the dusk sector (Holappa & Mursula, 2018). This is also supported by the fact that the westward electrojet is relatively strongly dependent on conductivity controlled by precipitating electrons (Østgaard et al., 2002) while the conductivity for the eastward electrojet is mainly controlled by solar illumination (Finch et al., 2008).

The physical mechanism of the B_y effect is still poorly understood. We note that a recent study (Reistad et al., 2020) gives evidence that the polar cap size in both hemispheres also shows an explicit B_y dependence, possibly indicating a stronger reconnection at the dayside magnetopause for $B_y > 0$ ($B_y < 0$) in NH (SH) winter. Reistad et al. (2020) also found that the B_y effect in polar cap area is equally strong in both hemispheres, which is also expected if IMF B_y indeed modulates the dayside reconnection rate and, thus, the global energy input into the magnetosphere. This paper is consistent with this mechanism as we found equally strong B_y effects in the precipitating electron fluxes in both hemispheres.

This paper gives strong evidence that ionospheric currents and related high-latitude geomagnetic activity are strongly modulated by IMF B_y-dependent fluxes of precipitating electrons. However, more research is needed for a better understanding of the chain of mechanisms connecting IMF B_y to particle precipitation and other magnetospheric and ionospheric phenomena.

Acknowledgments
We acknowledge the financial support by the Academy of Finland to the ReSoLVE Centre of Excellence (project 272157), to the postdoctoral researcher project of LH (322459), and to the PROSPECT project (321440). The solar wind data were downloaded from the OMNI2 database (http://omniweb.gsfc.nasa.gov/). All the original POES/MEPED energetic particle data used here are archived in the NOAA/NGDC dataserver (http://www.ngdc.noaa.gov/stp/satellite/poes/index.html).

References

Asikainen, T., & Mursula, K. (2013). Correcting the NOAA/MEPED energetic electron fluxes for detector efficiency and proton contamination. *Journal of Geophysical Research: Space Physics*, *118*, 6500–6510. https://doi.org/10.1002/jgra.50584

Asikainen, T., & Ruopsa, M. (2019). New homogeneous composite of energetic electron fluxes from POES satellites: 1. Correction for background noise and orbital drift. *Journal of Geophysical Research: Space Physics*, *124*, 1203–1221. https://doi.org/10.1029/2018JA026214

Connor, H. K., Raeder, J., Sibeck, D. G., & Trattner, K. J. (2015). Relation between cusp ion structures and dayside reconnection for four IMF clock angles: Openggcm-ltpt results. *Journal of Geophysical Research: Space Physics*, *120*, 4890–4906. https://doi.org/10.1002/2015JA021156

Fairfield, D. H., & Scudder, J. D. (1985). Polar rain: Solar coronal electrons in the Earth's magnetosphere. *Journal of Geophysical Research*, *90*(A5), 4055–4068.

Finch, I. D., Lockwood, M. L., & Rouillard, A. P. (2008). Effects of solar wind magnetosphere coupling recorded at different geomagnetic latitudes: Separation of directly-driven and storage/release systems. *Geophysical Research Letters*, *35*, L21105. https://doi.org/10.1029/2008GL035399

Friis-Christensen, E., Finlay, C. C., Hesse, M., & Laundal, K. M. (2017). Magnetic field perturbations from currents in the dark polar regions during quiet geomagnetic conditions. *Space Science Reviews*, *206*(1-4), 281–297.

Holappa, L., Gopalswamy, N., & Mursula, K. (2019). Explicit IMF by-effect maximizes at subauroral latitudes (dedicated to the memory of Eigil Friis-Christensen). *Journal of Geophysical Research: Space Physics*, *124*, 2854–2863. https://doi.org/10.1029/2018JA026285

Holappa, L., & Mursula, K. (2018). Explicit IMF B_y-dependence in high-latitude geomagnetic activity. *Journal of Geophysical Research: Space Physics*, *123*, 4728–4740. https://doi.org/10.1029/2018JA025517

Laitinen, T. V., Palmroth, M., Pulkkinen, T. I., Janhunen, P., & Koskinen, H. E. J. (2007). Continuous reconnection line and pressure-dependent energy conversion on the magnetopause in a global mhd model. *Journal of Geophysical Research*, *112*, A11201. https://doi.org/10.1029/2007JA012352

Lam, M. M., Horne, R. B., Meredith, N. P., Glauert, S. A., Moffat-Griffin, T., & Green, J. (2010). Origin of energetic electron precipitation $>$ 30 kev into the atmosphere. *Journal of Geophysical Research*, *115*, A00F08. https://doi.org/10.1029/2009JA014619

Liu, Z.-Q., Lu, J. Y., Kabin, K., Yang, Y. F., Zhao, M. X., & Cao, X. (2012). Dipole tilt control of the magnetopause for southward IMF from global magnetohydrodynamic simulations. *Journal of Geophysical Research*, *117*, A07207. https://doi.org/10.1029/2011JA017441

Meredith, N. P., Horne, R. B., Lam, M. M., Denton, M. H., Borovsky, J. E., & Green, J. C. (2011). Energetic electron precipitation during high-speed solar wind stream driven storms. *Journal of Geophysical Research*, *116*, A05223. https://doi.org/10.1029/2010JA016293

Newell, P. T., Sotirelis, T., Liou, K., Meng, C.-I., & Rich, F. J. (2007). A nearly universal solar wind-magnetosphere coupling function inferred from 10 magnetospheric state variables. *Journal of Geophysical Research*, *112*, A01206. https://doi.org/10.1029/2006JA012015

Østgaard, N., Vondrak, R. R., Gjerloev, J. W., & Germany, G. (2002). A relation between the energy deposition by electron precipitation and geomagnetic indices during substorms. *Journal of Geophysical Research*, *107*(A9), 1246. https://doi.org/10.1029/2001JA002003

Park, K. S., Ogino, T., & Walker, R. J. (2006). On the importance of antiparallel reconnection when the dipole tilt and IMF by are nonzero. *Journal of Geophysical Research*, *111*, A05202. https://doi.org/10.1029/2004JA010972

Pettigrew, E. D., Shepherd, S. G., & Ruohoniemi, J. M. (2010). Climatological patterns of high-latitude convection in the Northern and Southern Hemispheres: Dipole tilt dependencies and interhemispheric comparisons. *Journal of Geophysical Research*, *115*, A07305. https://doi.org/10.1029/2009JA014956

Reistad, J. P., Laundal, K. M., Ohma, A., Moretto, T., & Milan, S. E. (2020). An explicit IMF By dependence on solar wind-magnetosphere coupling. *Geophysical Research Letters*, *47*, e2019GL086062. https://doi.org/10.1029/2019GL086062

Shue, J.-H., Newell, P., Liou, K., & Meng, C.-I. (2001). Influence of interplanetary magnetic field on global auroral patterns. *Journal of Geophysical Research*, *106*(A4), 5913–5926. https://doi.org/10.1029/2000JA003010

Smith, A. R. A., Beggan, C. D., Macmillan, S., & Whaler, K. A. (2017). Climatology of the auroral electrojets derived from the along-track gradient of magnetic field intensity measured by POGO, Magsat, CHAMP, and Swarm. *Space Weather*, *15*, 1257–1269. https://doi.org/10.1002/2017SW001675

Sonnerup, B. U. O. (1974). Magnetopause reconnection rate. *Journal of Geophysical Research*, *79*(10), 1546–1549. https://doi.org/10.1029/JA079i010p01546

Thomas, E. G., & Shepherd, S. G. (2018). Statistical patterns of ionospheric convection derived from mid-latitude, high-latitude, and polar SuperDARN HF radar observations. *Journal of Geophysical Research: Space Physics*, *123*, 3196–3216. https://doi.org/10.1002/2018JA025280

Trattner, K. J., Petrinec, S. M., Fuselier, S. A., & Phan, T. D. (2012). The location of reconnection at the magnetopause: Testing the maximum magnetic shear model with THEMIS observations. *Journal of Geophysical Research*, *117*, A01201. https://doi.org/10.1029/2011JA016959

Vampola, A. L., & Gorney, D. J. (1983). Electron energy deposition in the middle atmosphere. *Journal of Geophysical Research*, *88*(A8), 6267–6274. https://doi.org/10.1029/JA088iA08p06267

Zhu, C. B., Zhang, H., Ge, Y. S., Pu, Z. Y., Liu, W. L., Wan, W. X., et al. (2015). Dipole tilt angle effect on magnetic reconnection locations on the magnetopause. *Journal of Geophysical Research: Space Physics*, *120*, 5344–5354. https://doi.org/10.1002/2015JA020989